

Shell-model study of quadrupole collectivity in light tin isotopes

L. Coraggio,¹ A. Covello,² A. Gargano,¹ N. Itaco,^{1,2} and T. T. S. Kuo³

¹*Istituto Nazionale di Fisica Nucleare, Complesso Universitario di Monte S. Angelo, Via Cintia - I-80126 Napoli, Italy*

²*Dipartimento di Fisica, Università di Napoli Federico II, Complesso Universitario di Monte S. Angelo, Via Cintia - I-80126 Napoli, Italy*

³*Department of Physics, SUNY, Stony Brook, New York 11794, USA*

(Received 20 February 2015; revised manuscript received 19 March 2015; published 10 April 2015)

A realistic shell-model study is performed for neutron-deficient tin isotopes up to mass $A = 108$. All shell-model ingredients, namely, two-body matrix elements, single-particle energies, and effective charges for electric quadrupole transition operators, have been calculated by way of the many-body perturbation theory, starting from a low-momentum interaction derived from the high-precision CD-Bonn free nucleon-nucleon potential. The focus has been on the enhanced quadrupole collectivity of these nuclei, which is testified by the observed large $B(E2; 0_1^+ \rightarrow 2_1^+)$ s. Our results give evidence of the crucial role played by the $Z = 50$ cross-shell excitations that need to be taken into account explicitly to obtain a satisfactory theoretical description of light tin isotopes. We find also that a relevant contribution comes from the calculated neutron effective charges, whose magnitudes exceed the standard empirical values. An original double-step procedure has been introduced to reduce effectively the model space in order to overcome the computational problem.

DOI: 10.1103/PhysRevC.91.041301

PACS number(s): 21.60.Cs, 23.20.Lv, 27.60.+j

Light tin isotopes have been an interesting laboratory since the early 1990s, when the experimental efforts toward the observation of the doubly closed ^{100}Sn became a sort of search for the “Holy Grail.” This has led to a certain amount of data that have improved our understanding of the structure of neutron-deficient isotopes, providing also a challenging ground for shell-model calculations. As a matter of fact, the study of light tin isotopes opened the way to a new generation of realistic shell-model calculations [1–3], an approach that has then flourished in the last two decades.

In the last few years, experimental interest has been renewed in studying these nuclei, especially with the help of intermediate-energy Coulomb-excitation experiments that are able to provide information on the electric quadrupole-excitation properties. In particular, in 2013 two papers reported about the measurement of the electric-quadrupole $0_1^+ \rightarrow 2_1^+$ transition rate in ^{104}Sn . The first work was performed at GSI [4], and the measured value is $B(E2; 0_1^+ \rightarrow 2_1^+) = 1000 \pm 400 e^2 \text{fm}^4$. This value fits well with the predictions of realistic shell-model calculations [5], where empirical effective charges have been employed, both when the model space is made up by only neutron orbitals above the ^{100}Sn core and when also proton excitations coming from the proton $0g_{9/2}$ orbital are included considering ^{90}Zr as a closed core.

The second paper reported the results of an experiment carried out at the National Superconducting Cyclotron Laboratory (NSCL) at Michigan State University [6]. In this work the measured value of the ^{104}Sn $B(E2; 0_1^+ \rightarrow 2_1^+)$ is larger, $1800 \pm 370 e^2 \text{fm}^4$, and disagrees more than 1σ with the value of Ref. [4]. Very recently, another measurement of this transition probability has been performed at RIKEN [7], wherein the result has been obtained from absolute Coulomb excitation cross sections. The reported value of the ^{104}Sn $B(E2; 0_1^+ \rightarrow 2_1^+)$ is $1730 \pm 280 e^2 \text{fm}^4$, consistent with the result of Ref. [6].

The value obtained in the last two papers is quite large and is not reproduced by shell-model calculations, even when proton degrees of freedom are explicitly taken into account.

In fact, various calculations [4–6,8–10] have been recently performed using ^{100}Sn and ^{90}Zr as closed cores, and they all predict $B(E2)$ values too small for the neutron-deficient tin isotopes as compared to the experimental ones. Moreover, no significant improvement is obtained by including also neutron excitations across the $N = 50$ shell closure, these excitations leading only to a slight increase of the $B(E2)$ s [4].

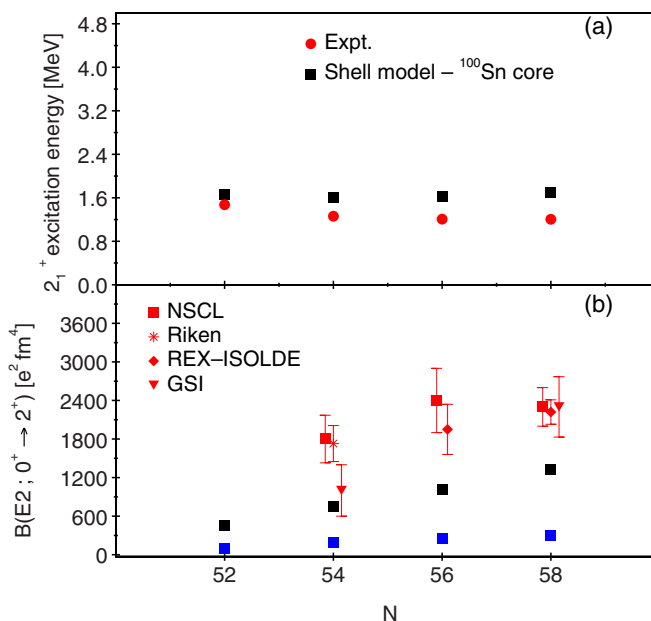


FIG. 1. (Color online) (a) Experimental [4–8,11] (red symbols) and calculated (black squares) excitation energies of the yrast $J^\pi = 2^+$ states and (b) $B(E2; 2_1^+ \rightarrow 0_1^+)$ transition rates for tin isotopes up to $N = 58$, when using neutron effective charges (I) reported in Table I. Blue squares refer to calculations with $e_n^{\text{emp}} = 0.5e$. Shell model calculations have been performed using only neutron degrees of freedom (see text for details).

TABLE I. Neutron effective charges of the electric quadrupole operator $E2$ for the model space with ^{100}Sn (I) and ^{88}Sr (II) as cores.

$n_a l_a j_a n_b l_b j_b$	$\langle a e_n b \rangle$ (I)	$\langle a e_n b \rangle$ (II)
$0g_{7/2}0g_{7/2}$	1.20	0.94
$0g_{7/2}1d_{5/2}$	1.27	0.96
$0g_{7/2}1d_{3/2}$	1.19	0.95
$1d_{5/2}1d_{5/2}$	0.81	0.94
$1d_{5/2}1d_{3/2}$	0.83	0.97
$1d_{5/2}2s_{1/2}$	0.79	0.79
$1d_{3/2}1d_{3/2}$	0.87	0.96
$1d_{3/2}2s_{1/2}$	0.85	0.79
$0h_{11/2}0h_{11/2}$	0.78	0.87

This background has been the main motivation to perform realistic shell-model calculations for neutron-deficient tin isotopes, using both the standard ^{100}Sn neutron-only model space and a larger one that includes $Z = 50$ cross-shell excitations with ^{88}Sr as an inert core. The main new elements of these calculations with respect to the previous ones are the inclusion of proton excitations from the $1p_{1/2}$ orbital and the use of microscopic effective charges, as well as an original procedure to reduce the large model space when considering ^{88}Sr as a closed core.

Another motivation is to revisit a region that, as mentioned before, has been for us the starting point for the investigation of the reliability of realistic shell-model calculations, going from the p -shell region up to nuclei around doubly closed ^{208}Pb core [12–17].

In our shell-model calculation we start from the high-precision nucleon-nucleon potential CD-Bonn [18], whose high-momentum repulsive components are smoothed out using the $V_{\text{low}-k}$ approach [19] so as to derive an effective Hamiltonian H_{eff} by way of the time-dependent perturbation theory [20,21]. The chosen cutoff momentum is $\Lambda = 2.6 \text{ fm}^{-1}$, and H_{eff} has been calculated including diagrams up to third order in $V_{\text{low}-k}$.

From the effective Hamiltonian both single-particle (SP) energies and two-body matrix elements (TBMEs) of the residual interaction have been obtained [22], and we have derived consistently the effective charges of the electric quadrupole operators at the same perturbative order.

At first, we consider a model space spanned by the five neutron $sdgh$ orbitals placed above doubly closed ^{100}Sn , so as to compare with previous realistic shell-model calculations. The calculated excitation energies of the yrast 2^+ states ($E_{2_1^+}^{\text{ex}}$) and the $B(E2; 0_1^+ \rightarrow 2_1^+)$ transition rates for tin isotopes up to $N = 58$ are reported in Fig. 1 and compared with the recent experimental data [4–8,11]. It can be seen that while the experimental behavior of both excitation energies and $B(E2)$ s is reproduced, the observed quadrupole collectivity is underestimated by our calculations, as evidenced by the fact that the predicted $E_{2_1^+}^{\text{ex}}$ s and $B(E2; 0_1^+ \rightarrow 2_1^+)$ s are larger and smaller, respectively, than the experimental ones. The $B(E2)$ s are too small notwithstanding the very large theoretical neutron effective charges e_n , as reported in Table I. It should be noted that the theory provides state-dependent effective charges, and the values relative

TABLE II. Proton effective charges of the electric quadrupole operator $E2$.

$n_a l_a j_a n_b l_b j_b$	$\langle a e_p b \rangle$
$0g_{9/2}0g_{9/2}$	1.62
$0g_{9/2}0g_{7/2}$	1.67
$0g_{9/2}1d_{5/2}$	1.60
$0g_{7/2}0g_{7/2}$	1.73
$0g_{7/2}1d_{5/2}$	1.74
$0g_{7/2}1d_{3/2}$	1.76
$1d_{5/2}1d_{5/2}$	1.73
$1d_{5/2}1d_{3/2}$	1.72
$1d_{5/2}2s_{1/2}$	1.76
$1d_{3/2}1d_{3/2}$	1.74
$1d_{3/2}2s_{1/2}$	1.76
$0h_{11/2}0h_{11/2}$	1.72

to the low-lying ($0g_{7/2}$) orbital exceed unity, being therefore quite different from the standard empirical one ($0.5e$).

We stress that this is a result at variance with those obtained in other regions. Actually, in our previous works for nuclei above ^{40}Ca [23], ^{48}Ca [15], and ^{132}Sn [24] cores, starting from the same realistic potential, we have obtained effective proton and neutron charges close to the empirical values. This seems to indicate that for nuclei around ^{100}Sn , relevant components of the real wave function lie outside the chosen model space, which induces a large renormalization of the theoretical effective electric-quadrupole operator.

For the sake of completeness, in Fig. 1 are also reported the results obtained with $e_n = 0.5e$ (blue squares), which do not differ too much from those reported in Ref. [6], where the effective interaction has been derived from the chiral N^3LO [25] and NNLO [26] NN potentials.

On the above grounds, we have considered a larger model space so as to take explicitly into account the $Z = 50$ cross-shell excitations of protons jumping from the $1p_{1/2}, 0g_{9/2}$ orbitals into the $sdgh$ ones. Within this large model space we have derived the effective Hamiltonian H_{eff}^{75} , where the superscript indicates the number of proton (seven) and neutron (five) orbitals we have considered. In Tables I and II are reported both theoretical neutron and proton effective charges, which are closer to the usual empirical values ($e_n^{\text{emp}} = 0.5\text{--}0.8e$, $e_p^{\text{emp}} = 1.5e$). However, some of the state-dependent e_n are close to unity, which may be considered an anomalous value with respect to the standard ones. As it could be expected, the enlargement of the model space provides wave functions closer to the real ones, even if the large e_n s indicate that relevant components are still missing.

The major difficulty with H_{eff}^{75} is that it cannot be diagonalized for any tin isotope with up-to-date shell-model codes. One has then to overcome the computational problem finding some way to reduce the dimensions of the matrices to be diagonalized, and consequently make the shell-model calculation feasible. This problem has been also faced in Ref. [5], where the shell-model calculations were performed allowing up to $4p\text{--}4h$ proton ^{90}Zr core excitations only.

In the present work, we have resorted for the first time to an approach which, by way of a unitary transformation of H_{eff}^{75} ,

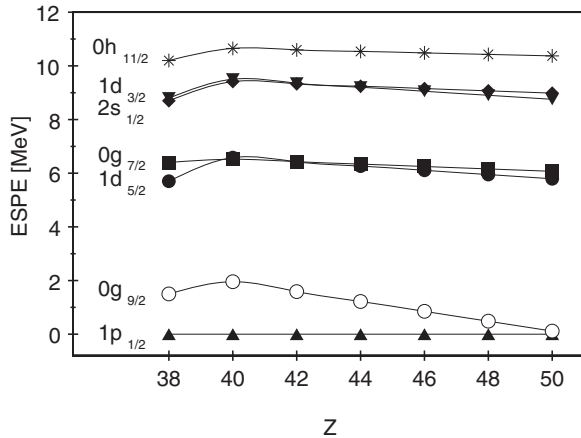


FIG. 2. Calculated proton effective single-particle energies of H_{eff}^{75} as a function of the atomic number Z .

leads to a new effective Hamiltonian defined in a truncated model space. The choice of the truncation of the model space is driven by the behavior, as a function of Z and N , of the proton and neutron effective single-particle energies (ESPEs) of the original Hamiltonian H_{eff}^{75} , so as to find out what are the most relevant degrees of freedom to describe the physics of light tin isotopes. To this end, we report in Figs. 2 and 3 the evolution of both proton and neutron ESPEs as a function of Z . From the inspection of Fig. 2, it can be observed that an almost constant energy gap provides a separation between the subspace spanned by the $1p_{1/2}, 0g_{9/2}, 1d_{5/2}, 0g_{7/2}$ proton orbitals and that spanned by the $2s_{1/2}, 1d_{3/2}, 0h_{11/2}$ ones. This leads to the conclusion that a reasonable truncation is to consider only the lowest four orbitals as proton model space.

On the neutron side, Fig. 3 gives evidence that the filling of the proton $0g_{9/2}$ orbital induces a relevant energy gap at $Z = 50$ between the $1d_{5/2}, 0g_{7/2}$ subspace and that spanned by the $2s_{1/2}, 1d_{3/2}, 0h_{11/2}$ orbitals. This gap, around 2.4 MeV, traces back to the tensor component of the proton-neutron interaction that is mainly responsible for the shell evolution [27]. Our calculated monopole component of the proton-neutron $0g_{9/2}, 0g_{7/2}$ interaction is -0.479 MeV.

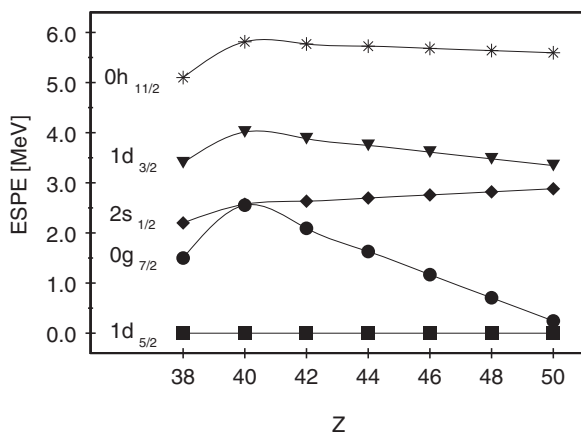


FIG. 3. Calculated neutron effective single-particle energies of H_{eff}^{75} as a function of Z .

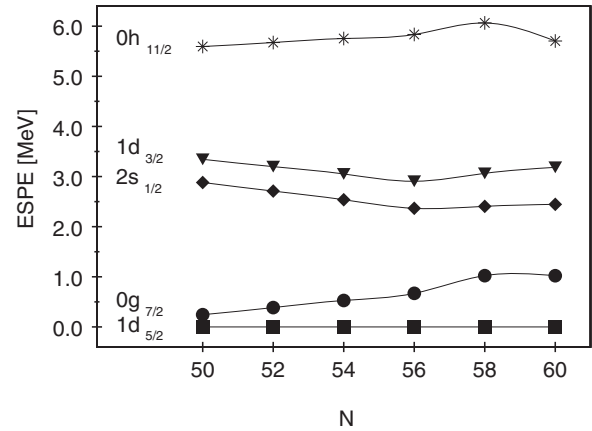


FIG. 4. Effective single-particle energies of tin isotopes as a function of N calculated with H_{eff}^{75} .

We, therefore, have deemed it reasonable that a neutron model space spanned only by the $1d_{5/2}, 0g_{7/2}$ orbitals may provide the relevant features of the physics of light tin isotopes. Moreover, if we consider the evolution of the neutron ESPE as a function of N (see Fig. 4), it can be observed that $2s_{1/2}, 1d_{3/2}, 0h_{11/2}$ orbitals start to play a more relevant role from ^{108}Sn on. Actually, the reduction of the energy gap between these orbitals and the $1d_{5/2}, 0g_{7/2}$ ones, and the progressive filling of the latter, may reduce the effectiveness of the truncated model space to describe the physics of tin isotopes above $N = 56$.

On these grounds, we have derived a new effective Hamiltonian H_{eff}^{42} , defined within a model space spanned only by the $1p_{1/2}, 0g_{9/2}, 1d_{5/2}, 0g_{7/2}$ proton and $1d_{5/2}, 0g_{7/2}$ neutron orbitals, by way of a unitary transformation of H_{eff}^{75} (see, for example, Refs. [28,29]).

It should be pointed out that we have applied this unitary transformation to the two valence-nucleon systems only, so that the energy spectra of ^{90}Zr , ^{90}Sr , and ^{90}Y are exactly the same when diagonalizing H_{eff}^{75} and H_{eff}^{42} . In order to obtain the same outcome for the eigenvalues of ^{102}Sn , besides H_{eff}^{42} , one should include effective many-body forces, which can only be obtained by diagonalizing H_{eff}^{75} for this nucleus. As already pointed out, this is unfeasible, so we have taken into account only TBME of H_{eff}^{42} .

It is obvious that the larger is the chosen subspace the smaller is the role of these effective many-body components. First of all, it may be worth verifying the reliability of our truncation scheme for tin isotopes. To this end we have derived another Hamiltonian, starting from H_{eff}^{75} , defined in the full $sdgh$ neutron model space but with the same proton model space of H_{eff}^{42} . This is the largest model space in which we can manage to diagonalize the shell-model Hamiltonian of ^{102}Sn . We dub this effective Hamiltonian H_{eff}^{45} , and in Fig. 5 we compare the low-energy spectra of ^{102}Sn obtained by means of H_{eff}^{45} and H_{eff}^{42} with the observed one [30].

It can be noted that H_{eff}^{45} is able to reproduce quite well the experimental spectrum, and that the spectrum calculated with H_{eff}^{42} is in good agreement with results obtained with H_{eff}^{45} .

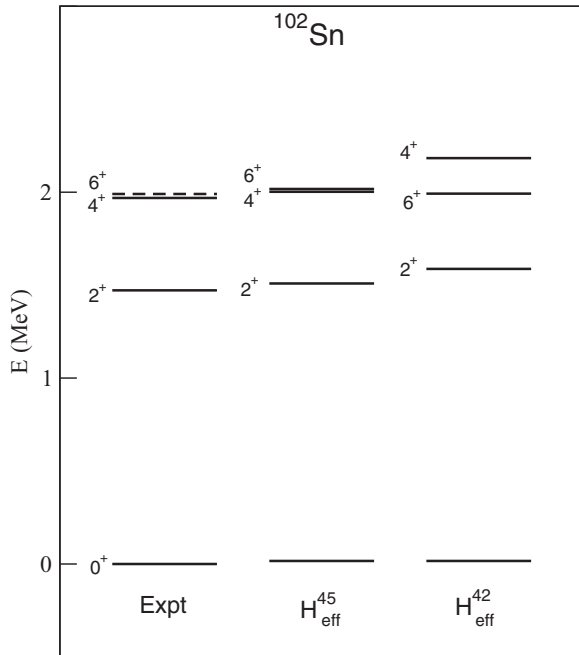


FIG. 5. Experimental [30] and theoretical spectra of ^{102}Sn calculated with H_{eff}^{45} and H_{eff}^{42} (see text for details).

It is very relevant, for the subject of our study, to point out that the $B(E2; 0_1^+ \rightarrow 2_1^+)$ calculated with H_{eff}^{42} is $1065 e^2 \text{fm}^4$, very close to the value of $1135 e^2 \text{fm}^4$ obtained with H_{eff}^{45} . This supports the adequacy of our truncation scheme when using H_{eff}^{42} and increasing the number of valence neutrons. This is an important result since our calculations, performed by way of the Oslo shell-model code [31], cannot be extended to heavier tin isotopes using H_{eff}^{45} .

In Fig. 6 we report the experimental $E_{2_1^+}^{\text{ex}}$ and $B(E2; 0_1^+ \rightarrow 2_1^+)$ (red symbols) for the tin isotopes up to $N = 58$, and

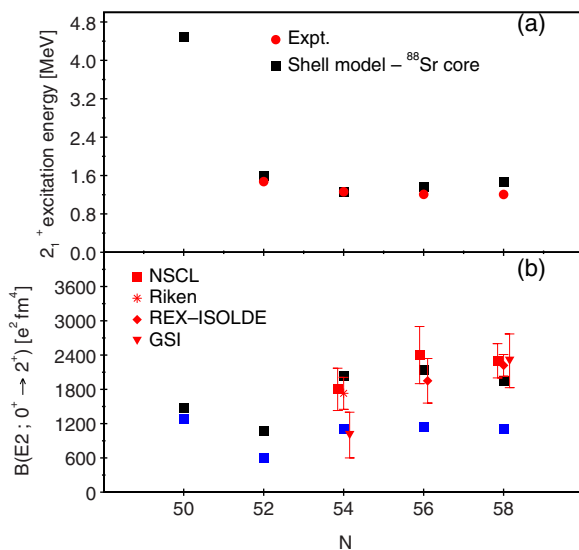


FIG. 6. (Color online) Same as in Fig. 1, but with shell-model results obtained with H_{eff}^{42} . Blue squares refer to calculations with $e_n^{\text{emp}} = 0.5, e_p^{\text{emp}} = 1.5$.

TABLE III. Occupation numbers of proton $1p_{1/2}, 0g_{9/2}, 0g_{7/2}, 1d_{5/2}$ of $^{102-108}\text{Sn}$ $J = 0_1^+, 2_1^+$ state, calculated with model space III (see text for details).

Orbital	^{102}Sn	^{104}Sn	^{106}Sn	^{108}Sn	
		$J = 0^+$			
$\pi 1p_{1/2}$	1.97	1.98	1.98	1.98	
$\pi 0g_{9/2}$	9.55	9.38	9.36	9.38	
$\pi 0g_{7/2}$	0.26	0.28	0.27	0.25	
$\pi 1d_{5/2}$	0.22	0.37	0.40	0.39	
		$J = 2^+$			
$\pi 1p_{1/2}$	1.98	1.98	1.98	1.98	
$\pi 0g_{9/2}$	9.50	9.23	9.21	9.27	
$\pi 0g_{7/2}$	0.25	0.28	0.27	0.24	
$\pi 1d_{5/2}$	0.28	0.51	0.54	0.51	

compare them with the results obtained using H_{eff}^{42} (black squares). We have also included our prediction for the closed shell ^{100}Sn , where only proton degrees of freedom are taken into account. As in Fig. 1, we have included the calculated $B(E2)$ s when using $e_n^{\text{emp}} = 0.5e, e_p^{\text{emp}} = 1.5e$.

We see that the shell-model calculations with H_{eff}^{42} are able to reproduce quite well the experimental $E_{2_1^+}^{\text{ex}}$ and, when employing the theoretical effective charges, the $B(E2; 0_1^+ \rightarrow 2_1^+)$ up to $A = 106$ and, consequently, the onset of collectivity from ^{102}Sn on, driven by the $Z = 50$ cross-shell excitations. As a matter of fact, the wave functions evidence a depletion of the proton $0g_{9/2}$ orbital from ^{102}Sn to ^{106}Sn , as testified by the occupation numbers reported in Table III. It is worth pointing out that the agreement with experiment for ^{108}Sn deteriorates with respect to lighter isotopes, owing to the fact that, as already mentioned, the influence of neutron $1d_{3/2}, 2s_{1/2}, 0h_{11/2}$ orbitals starts to play a non-negligible role.

In summary, we have performed a shell-model study of light tin isotopes starting from a realistic NN potential, where all results have been obtained without resorting to any empirical parameter. The main features of present work may be itemized as follows:

- (1) We have confirmed the crucial role of the $Z = 50$ cross-shell excitations to obtain a satisfactory description of tin isotopes. This implies the use of a large shell-model space including both proton and neutron orbitals.
- (2) We have followed an original double-step approach to reduce the computational complexity of the shell-model problem. This is based on the study of the ESPEs of the large-scale Hamiltonian, so as to identify the most relevant degrees of freedom to be taken into account in the construction of a truncated shell-model Hamiltonian. To this end, a unitary transformation is employed.
- (3) We have highlighted the role of theoretical effective charges in reproducing the quadrupole collectivity of the $B(E2)$ s.
- (4) We have presented some predictions for $^{100,102}\text{Sn}$ spectroscopic properties, which may provide guidance for future experiments.

- [1] T. Engeland, M. Hjorth-Jensen, A. Holt, and E. Osnes, *Phys. Rev. C* **48**, R535(R) (1993).
- [2] M. Hjorth-Jensen, T. T. S. Kuo, and E. Osnes, *Phys. Rep.* **261**, 125 (1995).
- [3] F. Andreozzi, L. Coraggio, A. Covello, A. Gargano, T. T. S. Kuo, Z. B. Li, and A. Porrino, *Phys. Rev. C* **54**, 1636 (1996).
- [4] G. Guastalla, D. D. DiJulio, M. Górska, J. Cederkäll, P. Boutachkov, P. Golubev, S. Pietri, H. Grawe, F. Nowacki, K. Sieja *et al.*, *Phys. Rev. Lett.* **110**, 172501 (2013).
- [5] A. Banu, J. Gerl, C. Fahlander, M. Górska, H. Grawe, T. R. Saito, H.-J. Wollersheim, E. Caurier, T. Engeland, A. Gniady *et al.*, *Phys. Rev. C* **72**, 061305 (2005).
- [6] V. M. Bader, A. Gade, D. Weisshaar, B. A. Brown, T. Baugher, D. Bazin, J. S. Berryman, A. Ekström, M. Hjorth-Jensen, S. R. Stroberg *et al.*, *Phys. Rev. C* **88**, 051301 (2013).
- [7] P. Doornenbal, S. Takeuchi, N. Aoi, M. Matsushita, A. Obertelli, D. Steppenbeck, H. Wang, L. Audirac, H. Baba, P. Bednarczyk *et al.*, *Phys. Rev. C* **90**, 061302 (2014).
- [8] C. Vaman, C. Andreoiu, D. Bazin, A. Becerril, B. A. Brown, C. M. Campbell, A. Chester, J. M. Cook, D. C. Dinca, A. Gade *et al.*, *Phys. Rev. Lett.* **99**, 162501 (2007).
- [9] C. Qi and Z. X. Xu, *Phys. Rev. C* **86**, 044323 (2012).
- [10] T. Bäck, C. Qi, B. Cederwall, R. Liotta, F. Ghazi Moradi, A. Johnson, R. Wyss, and R. Wadsworth, *Phys. Rev. C* **87**, 031306 (2013).
- [11] A. Ekström, J. Cederkäll, C. Fahlander, M. Hjorth-Jensen, F. Ames, P. A. Butler, T. Davinson, J. Eberth, F. Fincke, A. Görge *et al.*, *Phys. Rev. Lett.* **101**, 012502 (2008).
- [12] L. Coraggio, A. Covello, A. Gargano, N. Itaco, and T. T. S. Kuo, *J. Phys. G* **27**, 2351 (2001).
- [13] L. Coraggio, A. Covello, A. Gargano, and N. Itaco, *Phys. Rev. C* **81**, 064303 (2010).
- [14] L. Coraggio, A. Covello, A. Gargano, N. Itaco, D. R. Entem, T. T. S. Kuo, and R. Machleidt, *Phys. Rev. C* **75**, 024311 (2007).
- [15] L. Coraggio, A. Covello, A. Gargano, and N. Itaco, *Phys. Rev. C* **89**, 024319 (2014).
- [16] L. Coraggio, A. Covello, A. Gargano, and N. Itaco, *Phys. Rev. C* **80**, 021305 (2009).
- [17] L. Coraggio, A. Covello, A. Gargano, N. Itaco, and T. T. S. Kuo, *Phys. Rev. C* **60**, 064306 (1999).
- [18] R. Machleidt, *Phys. Rev. C* **63**, 024001 (2001).
- [19] S. Bogner, T. T. S. Kuo, L. Coraggio, A. Covello, and N. Itaco, *Phys. Rev. C* **65**, 051301(R) (2002).
- [20] T. T. S. Kuo, S. Y. Lee, and K. F. Ratcliff, *Nucl. Phys. A* **176**, 65 (1971).
- [21] L. Coraggio, A. Covello, A. Gargano, N. Itaco, and T. T. S. Kuo, *Prog. Part. Nucl. Phys.* **62**, 135 (2009).
- [22] L. Coraggio, A. Covello, A. Gargano, N. Itaco, and T. T. S. Kuo, *Ann. Phys.* **327**, 2125 (2012).
- [23] L. Coraggio, A. Covello, A. Gargano, and N. Itaco, *Phys. Rev. C* **80**, 044311 (2009).
- [24] L. Coraggio, A. Covello, A. Gargano, N. Itaco, and T. T. S. Kuo, *Phys. Rev. C* **80**, 044320 (2009).
- [25] D. R. Entem and R. Machleidt, *Phys. Rev. C* **68**, 041001(R) (2003).
- [26] A. Ekström, G. Baardsen, C. Forssén, G. Hagen, M. Hjorth-Jensen, G. R. Jansen, R. Machleidt, W. Nazarewicz, T. Papenbrock, J. Sarich *et al.*, *Phys. Rev. Lett.* **110**, 192502 (2013).
- [27] T. Otsuka, T. Suzuki, R. Fujimoto, H. Grawe, and Y. Akaishi, *Phys. Rev. Lett.* **95**, 232502 (2005).
- [28] K. Suzuki, R. Okamoto, H. Kumagai, and S. Fujii, *Phys. Rev. C* **83**, 024304 (2011).
- [29] K. Suzuki, H. Kumagai, R. Okamoto, and M. Matsuzaki, *Phys. Rev. C* **89**, 044003 (2014).
- [30] Data extracted using the NNDC On-line Data Service from the ENSDF database, file revised as of September 12, 2013.
- [31] T. Engeland, the Oslo shell-model code 1991–2006 (unpublished).